

SHORT REPORT*Special Technologies in Omics of the Cardiovascular System*

Quantifying cardiovascular autonomic aging with machine learning

Andy Schumann,¹ Yubraj Gupta,¹ Maria Geisler,¹ Feliberto de la Cruz,¹ Denis Gerstorf,² Ilja Demuth,^{3,4} Maja Olecka,⁵ Christian Gaser,^{6,7,8} and Karl-Jürgen Bär¹

¹Lab for Autonomic Neuroscience, Imaging and Cognition (LANIC), Department of Psychosomatic Medicine and Psychotherapy, Jena University Hospital, Jena, Germany; ²Department of Psychology, Humboldt-Universität zu Berlin, Berlin, Germany; ³Department of Endocrinology and Metabolic Diseases (including Division of Lipid Metabolism), Biology of Aging working group, Charité – Universitätsmedizin Berlin, Corporate Member of Freie Universität Berlin and Humboldt-Universität zu Berlin, Berlin, Germany; ⁴Regenerative Immunology and Aging, BIH Center for Regenerative Therapies, Charité – Universitätsmedizin Berlin, Corporate Member of Freie Universität Berlin, Humboldt-Universität zu Berlin, Berlin Institute of Health, Berlin, Germany; ⁵Hoffmann Lab, Leibniz Institute on Aging – Fritz Lipmann Institute (FLI), Jena, Germany; ⁶Department of Neurology, Jena University Hospital, Jena, Germany; ⁷Department of Psychiatry and Psychotherapy, Jena University Hospital, Jena, Germany; and ⁸German Center for Mental Health (DZPG), Berlin, Germany

Abstract

Machine learning has become an important tool in precision medicine and aging research. We introduce the cardiovascular autonomic age (CAA) gap, a novel metric quantifying the deviation between machine learning-estimated biological age and chronological age based on autonomic cardiovascular function. High-resolution electrocardiograms and continuous blood pressure recordings at rest were collected from 1,060 healthy individuals. From these signals, 29 autonomic indices were derived, including time-, frequency-, and symbol-domain heart rate variability, cardiovascular coupling, pulse wave dynamics, and QT interval features. A Gaussian process regression model was trained on 879 participants to estimate biological age, yielding the CAA. The deviation between CAA and chronological age defined the CAA gap, which was evaluated in two test sets stratified by cardiovascular risk (CVR) using the Framingham risk score. At a 0.5% threshold, the high-CVR group showed a markedly increased CAA gap (+11 yr), whereas the low-CVR group demonstrated a slightly negative gap (-1 yr). In the high-risk group, the slope of predicted versus actual age suggested accelerated physiological aging. CAA correlated positively with the Framingham risk score ($r = 0.42, P < 0.001$), and the CAA gap correlated with deviation from normative risk ($r = 0.31, P = 0.002$). Across thresholds, elevated CAA in the high-CVR group was consistently observed, with moderate effect sizes ranging from 0.32 to 0.46. These findings suggest that the CAA gap may serve as a sensitive and interpretable indicator of cardiovascular risk and aging, with potential relevance for early detection and longitudinal assessment.

NEW & NOTEWORTHY The cardiovascular autonomic age (CAA) gap is a new machine learning-based marker that reveals when the body ages faster than the clock. Using resting-state cardiovascular recordings from 1,000 + participants, we show that individuals with higher cardiovascular risk exhibit accelerated autonomic aging. The CAA gap could become a sensitive, interpretable tool for early detection and long-term monitoring.

biological aging; cardiovascular risk; Framingham risk score; heart rate variability; precision medicine

INTRODUCTION

Aging profoundly affects cardiovascular health and remains the leading contributor to morbidity and mortality worldwide. Understanding how aging influences cardiac and vascular regulation is essential for identifying early markers of cardiovascular dysfunction and improving prevention strategies. As global life expectancy increases, the burden of age-related cardiovascular diseases, such as hypertension, coronary artery

disease, and heart failure, continues to rise, highlighting the importance of differentiating healthy from pathological aging (1). Although chronological age is a major determinant of cardiovascular risk (CVR), it does not fully capture the biological variability in how individuals age.

Age-related changes in the cardiovascular system are widespread, affecting myocardial contractility, diastolic relaxation, and chronotropic responsiveness, as well as reducing vascular elasticity and endothelial function (2).



Correspondence: A. Schumann (andy.schumann@med.uni-jena.de).

Submitted 8 September 2025 / Revised 30 September 2025 / Accepted 17 October 2025



These structural and functional alterations are accompanied by a shift toward sympathetic dominance and reduced parasympathetic activity, leading to increased resting heart rate, blood pressure, and cardiovascular stress. A decreased sensitivity of vagal reflexes, such as respiratory sinus arrhythmia, leads to diminished heart rate variability (HRV) in elderly individuals (3–5). The baroreflex feedback loop decelerating heart rate in response to rising blood pressure is progressively reduced with age, contributing to blood pressure variability and adverse cardiovascular outcomes (6–10). Autonomic imbalance also affects ventricular repolarization, increasing QT interval variability and arrhythmic risk (11). Together, these alterations diminish cardiovascular resilience and increase susceptibility to disease.

Autonomic dysfunction has increasingly been recognized not only as a correlate but also as an early marker of elevated cardiovascular risk (12). Reduced heart rate variability (HRV) has been associated with increased all-cause and cardiac mortality across populations (13–15). Hillebrand et al. (16) reported that healthy participants with diminished resting HRV had a 32%–45% higher risk of experiencing a first cardiovascular event over up to 15 years of follow-up. Independent evidence implicates sympathetic overactivity in the pathogenesis of hypertension, vascular dysfunction, and adverse cardiovascular outcomes (17). These findings support the view that autonomic functional alterations often precede structural cardiovascular changes and may serve as early, mechanistically informative biomarkers for identifying individuals at heightened cardiovascular risk.

However, conventional cardiovascular risk assessments such as the Framingham risk score primarily capture cumulative exposure to static risk factors (e.g., cholesterol, blood pressure, diabetes, and smoking) and do not reflect short-term physiological adaptability. Based on a cohort of 8,491 Framingham participants, sex-specific risk functions were derived to estimate 10-yr atherosclerotic cardiovascular risk (18). Independent studies have confirmed that laboratory based and body mass index (BMI)-based scores have similar predictive accuracy for fatal and nonfatal cardiovascular events (19, 20). Previous research has shown that individuals in high Framingham risk categories develop cardiovascular disease about 8–10 years earlier than those at low risk (18, 21), and obesity-based stratifications predict earlier onset by 5–10 years (22). Although such risk assessments effectively capture long-term exposure, incorporating additional functional autonomic and subclinical markers may improve the early detection of accelerated cardiovascular aging before overt diseases develop.

Machine learning (ML) can be applied to track age-related changes in specific organ systems, helping to characterize normal, healthy aging processes and generate individualized age estimates. When an individual's estimated age, derived from a machine learning model, exceeds their actual chronological age, it may indicate accelerated aging and elevated health risk. Such "risk ages" or age equivalents can enhance communication with patients by presenting risk in a relatable and understandable way, potentially improving adherence to lifestyle modifications and pharmacotherapies (23). Although some age equivalents appear

to be quite common for risk prediction in a clinical context, the potential of machine learning to enhance, complement, or outperform them has not been fully leveraged. Existing markers such as "Heart Age," "Vascular Age," "Arterial Age," or "Coronary Age" are based on a few specific cardiovascular risk factors that are rather easy to assess and used in clinical routine (18, 24–27).

As a first step toward harnessing the potential of machine learning, we recently developed a model to estimate age based on cardiovascular function (28). In total, 29 cardiovascular indices were estimated as input features to the age-prediction model, including heart rate variability, blood pressure variability, baroreflex function, pulse wave dynamics, and QT interval characteristics. Four approaches were tested to estimate the chronological age of healthy individuals: 1) relevance vector regression, 2) Gaussian process regression (GPR), 3) support vector regression, and 4) linear regression. Through a fivefold cross-validation process, the GPR model demonstrated the best performance in estimating chronological age, achieving a high correlation and a mean absolute error of 5.6 yr. Interestingly, the estimated age of individuals with obesity (body mass index $> 30 \text{ kg/m}^2$) was markedly higher by up to 6 yr on average compared with normal-weight participants indicating an advanced cardiovascular aging in this group.

This study investigates whether the prediction error of the healthy aging ML model (age gap) is associated with altered cardiovascular risk in these individuals. Using the Framingham risk score, we estimated 10-years cardiovascular risk in a sample of healthy individuals. We identified participants with higher and with lower risk compared with the age- and sex-dependent normative risk. The cardiovascular autonomic age (CAA) gap was assessed as a deviation from healthy aging and compared between high- and low-risk groups.

MATERIALS AND METHODS

Participants

We investigated data of 1,060 healthy individuals recorded in our laboratory. The majority of datasets have been made publicly available already (29). None of the subjects had any history of a neurological or psychiatric disorder. Exclusion criteria were any medical conditions, illegal drugs, or medications potentially influencing cardiovascular function. Thorough physical examination, resting electrocardiogram, and routine laboratory parameters (electrolytes, basic metabolic panel, and blood count) had to be without any pathological finding. All participants provided written informed consent before participating in the study. The study protocol was approved by the Ethics Committee of the University Hospital of Jena.

Cardiovascular Risk Estimation

We used the updated Framingham risk calculation model to predict the 10-yr risk of atherosclerotic cardiovascular disease, including coronary heart disease, stroke, peripheral vascular disease, and heart failure (18). Cardiovascular risk (CVR) was estimated based on age, sex, systolic blood pressure

(SBP), BMI, hypertension or diabetes diagnosis, smoking status, and current use of antihypertensive medications. The calculation algorithm is publicly available at the Framingham Heart Study website (<https://www.framinghamheartstudy.org/fls-risk-functions/cardiovascular-disease-10-year-risk/>). CVR estimates range from 0.3% to over 30%, with a practical upper limit of 98.5%. In addition, normative risk at a given age can be approximated by assuming an untreated SBP of 125 mmHg, BMI of 22.5 kg/m², a nonsmoker and non-diabetic (18).

Training and Testing Samples

Of the 1,060 individuals in total, 181 participants formed the testing sets, as they had sufficient information to calculate the Framingham risk score (requiring age between 30 yr and 74 yr, as well as complete data on smoking status, hypertension treatment, body mass index, and diabetes diagnosis). The remaining 879 individuals (351 men, 528 women; mean age 31.8 ± 14 yr) were used for training the model.

Defining Test Samples according to Cardiovascular Risk

According to the Framingham risk score, we separated participants of the testing sample into high- and low-cardiovascular risk groups (high CVR, low CVR). Since no clinically validated cutoff exists, we applied varying thresholds relative to the normative population risk. Thresholds ranged from 0% (where any individual with a risk above the normative risk was categorized as high CVR, and below as low CVR) up to 0.6% (where individuals with a risk at least 0.6% higher or 0.6% lower than the normative risk were classified as high and low CVR, respectively). We randomly sampled 50 individuals into both the high- and low-CVR test sets beyond the threshold (0, 0.4, 0.5, and 0.6%), with the remaining data used for validation ($n = 81$). We report in more detail one exemplary run using 0.5% as a threshold to identify low- and high-CVR individuals.

Data Acquisition

Continuous noninvasive blood pressure and electrocardiogram (ECG) were acquired simultaneously over 20 min using either a Task Force Monitor (TFM, CNSystems Medizintechnik GmbH, Graz, Austria) or MP150 (BIOPAC Systems Inc., Goleta, CA). Participants were in a supine position under well-controlled resting conditions in our laboratory. The assessment took place in a completely quiet and fully shaded room, with a constant illumination level. Following usual practice, the first 5 min were excluded from the analysis.

Feature Extraction

From these signals, we estimated 29 cardiovascular features including time, frequency, and symbol domain heart rate variability, cardiovascular parameters, pulse wave dynamics, and QT interval characteristics. Mean heart rate, root mean square of successive beat-to-beat intervals (BBI), standard deviation of BBI, low- and high-frequency power and their ratio (30), deceleration capacity (31), Rényi entropy with base one fourths (32), sample entropy (33), and compression entropy (34) were derived from BBI time series. Mean and standard deviation of corrected QT intervals (35) and the QT variability index were estimated (36). Mean and

standard deviation of systolic and diastolic blood pressure (DBP) values per heart beat interval were extracted (37). Pulse pressure was calculated as difference between SBP and DBP. Using the sequence method, baroreflex sensitivity was calculated as marker of bradycardic changes due to blood pressure increases (38). As a spectral method to assess baroreflex function, the cardiovascular coherence in the low- and high-frequency bands was estimated (39). Nonlinear coupling was assessed as the proportion of symmetric symbolic words from joint symbolic dynamics (40). Mean values and standard deviation of the pulse transit time, pulse rise time, pulse wave velocity (41), as well as the average delay of dicrotic notch to pulse maximum. A full list of cardiovascular indices is reported in the Supplemental Table S1.

Feature Selection and Scaling

To reduce redundancy and retain only informative features, we applied a two-step procedure based on variance inflation factor (VIF) and Pearson correlation. First, we iteratively removed variables with a VIF > 10 . Second, we computed pairwise Pearson correlation coefficients among all remaining features and from each pair with $r > 0.8$, we removed the feature that had the higher VIF. This procedure reduced the final feature set to 19 variables. All features were then standardized using *z*-score transformation (zero mean, unit variance) with the *StandardScaler* from scikit-learn, fitted on the training set and applied to all testing data to ensure consistent scaling and prevent data leakage.

Cardiovascular Autonomic Age Estimation

We applied machine learning to estimate effects of healthy cardiovascular aging based on 19 cardiovascular autonomic indices. The CAA gap represents the deviation between the estimated age from this model and people's chronological age. A positive age gap indicates advanced aging relative to one's chronological age, whereas a negative gap suggests delayed aging processes. A GPR model with a squared exponential kernel radial basis function (RBF) and a constant basis function was applied and derived from our existing model (28). Hyperparameters were optimized by grid search with cross-validation during training the model (*GridSearchCV*), resulting in a constant kernel variance of 1.1, an RBF length scale of 4.1, and a noise level of $\alpha = 0.13$. The final model was implemented with normalization of the output variable and 10 optimizer restarts to ensure stability.

We corrected the model output for a potential linear dependency of the estimated on the chronological age (age bias) by fitting a linear regression model in the validation sample (42). The age predictions in the high- and low-CVR groups were corrected for that bias using the estimated slope and intercept (43).

Feature Importance

To identify the most influential cardiovascular features contributing to the age predictions, we used the SHapley Additive exPlanation (SHAP) algorithm (44). SHAP analysis was performed in the entire test set of 181 healthy controls. Absolute SHAP values were extracted using a *KernelExplainer* and averaged to evaluate importance of each input feature.

Statistical Analysis

Differences between estimated age and chronological age were compared between participants with low and high CVR, using varying thresholds relative to the normative risk (0, 0.4, 0.5, and 0.6%). For each threshold, we randomly sampled $n = 50$ individuals meeting the respective risk criterion. This procedure was repeated 50 times to assess Cohen's d effect sizes (45) as a function of the applied threshold.

For one run using a threshold of 0.5%, we additionally report descriptive characteristics of the groups as well as the CAA gap. The association between the CAA and Framingham risk score across both test groups was examined using Pearson correlation. Comparisons of individual risk factors were performed with independent t tests for continuous variables and χ^2 tests for dichotomous variables.

The accuracy of age estimation was assessed in the validation sample using mean absolute error (MAE) and root mean squared error (RMSE).

RESULTS

A total of 29 parameters were extracted from resting recordings of noninvasive continuous blood pressure recordings and high-resolution electrocardiograms of each subject. After feature selection, 19 features were fed into a GPR model to estimate cardiovascular age (see Fig. 1).

In the validation sample, the model demonstrated a high concordance with chronological age, achieving a MAE = 6.04 yr and a RMSE = 8.97 yr. To identify the key contributors to age estimation, we calculated SHAP values (see Fig. 2). The most important features were pulse reflection time, pulse transit time, baroreflex sensitivity, and mean heart rate.

Age Estimates in Participants with Low- and High-Cardiovascular Risk

The Gaussian process framework was used to estimate the CAA gap as a deviation from normal healthy aging. The model

was trained on 879 individuals and applied to two groups: 1) healthy participants with high CVR and 2) those with low CVR. In this example, a threshold of 5% deviation from the normative risk was used to define high CVR (individual risk $>5\%$ above normative risk) and low CVR (individual risk $>5\%$ below normative risk). The characteristics of both groups are summarized in Table 1. As expected, the Framingham risk score was significantly higher in the high-CVR group, whereas normative risk estimates remained similar between the two groups. The high-CVR group had a higher prevalence of smokers and a higher BMI as well as increased SBP compared with the low CVR group. In contrast, self-reported exercise levels and the presence of depressive symptoms did not differ significantly between the groups.

High-CVR individuals had a significantly higher CAA gap ($+11.1 \pm 14.4$ yr) compared with low-CVR group (-0.9 ± 15.7 yr, $P = 0.0003$; Fig. 3, A and B). In the low-CVR group, cardiovascular age estimates closely tracked chronological age, with a near-unity regression slope ($m = 0.94$) and a slight positive offset (intercept = 2.3 yr). In contrast, the high-CVR group exhibited a steeper slope ($m = 1.26$) and a slight negative offset (intercept = -2.4 yr), consistent with accelerated aging, although the difference between slopes was not statistically significant ($P = 0.178$).

Effect size analysis across varying thresholds for defining high versus low CVR showed robust group differences, with average Cohen's d values ranging from 0.32 to 0.46 (Fig. 3C). The CAA across both groups was positively correlated with the Framingham risk score ($r = 0.42$, $P < 0.001$; Fig. 3D). In addition, the CAA gap was correlated with the deviation of an individual's Framingham risk score from normative risk ($r = 0.31$, $P = 0.002$; Fig. 3E).

DISCUSSION

Artificial intelligence has become an integral part of daily life, and machine learning (ML) is set to transform the medical and healthcare industries (46, 47). ML offers significant opportunities to enhance risk stratification, diagnostic classification,

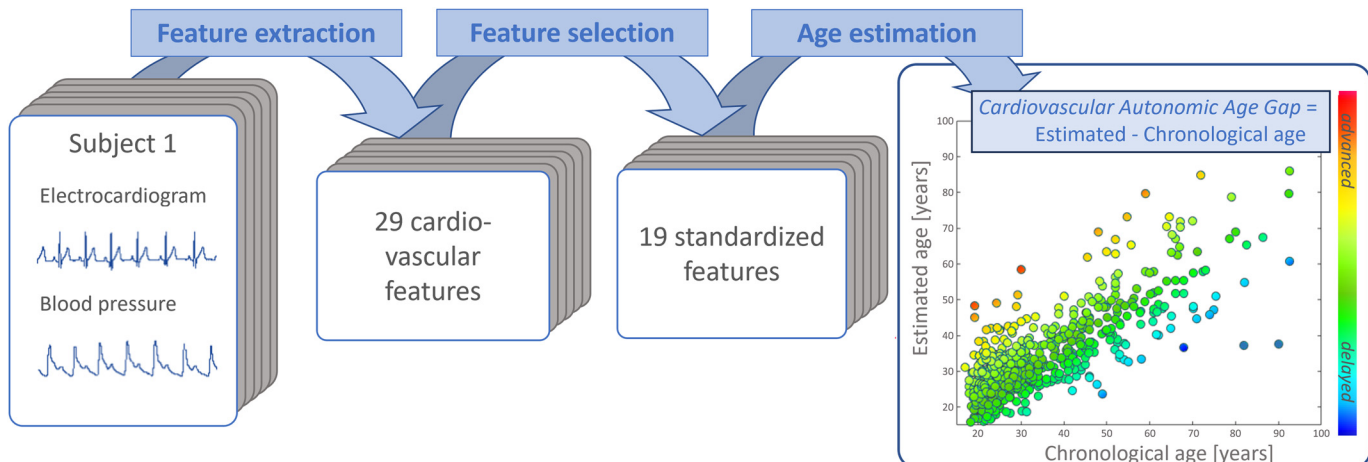


Figure 1. The framework for cardiovascular autonomic age gap estimation based on cardiovascular data. In total, 29 indices were extracted from resting recordings of blood pressure and electrocardiograms. Nineteen meaningful features were used as input to the model. Machine learning (Gaussian process regression model) was used to estimate age on the basis of these indices. The relation of estimated age and chronological age is depicted on the right side. The cardiovascular autonomic age gap is the difference between estimated and chronological age.

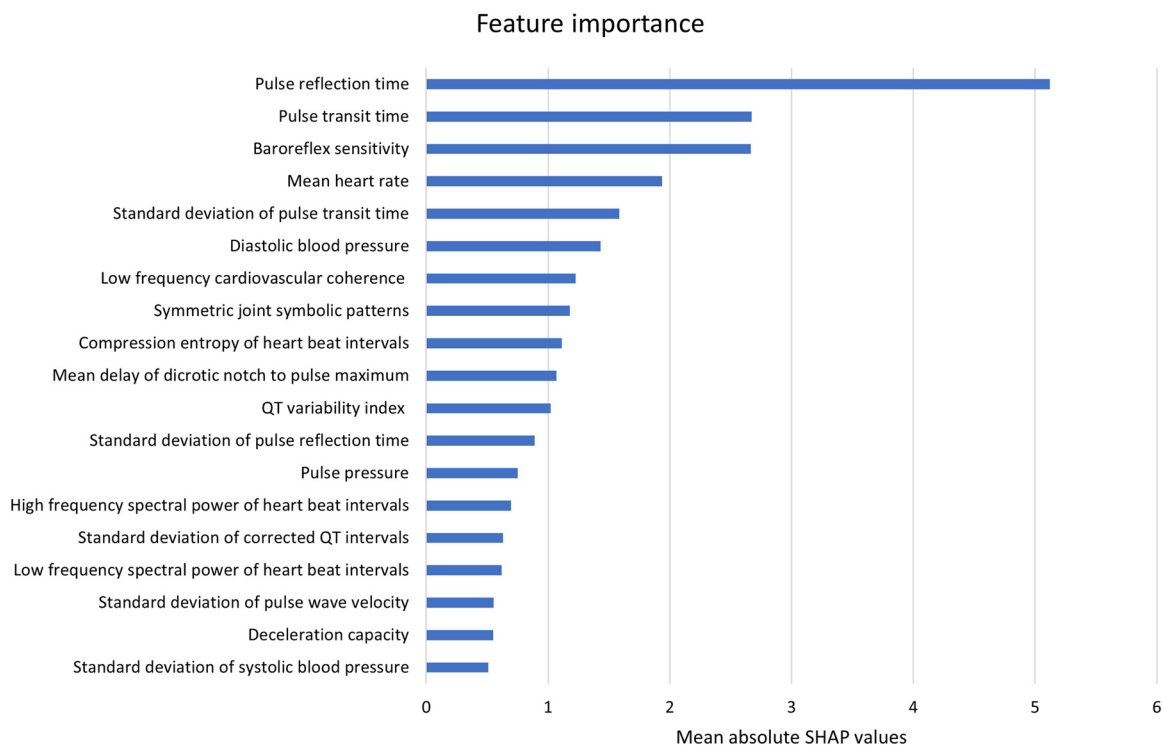


Figure 2. Averaged absolute SHAP values of cardiovascular autonomic features that were fed into the age estimation model. SHAP, SHapley Additive exPlanation.

and patient subgroup identification, among other applications (48). One notable application of ML is the quantification of aging effects based on biological data, which has provided insights into the aging processes of different organ systems (49–51). Research suggests that these biological markers that track the aging process, the “aging clocks,” progress at individual rates, which makes them a promising tool for precision medicine (52, 53).

In this study, we propose an ML-based framework to evaluate aging effects on cardiovascular autonomic regulation using a comprehensive set of biomarkers. CAA quantifies the

deviation between ML-predicted age and chronological age, providing insights into cardiovascular aging. We tested various ML algorithms to estimate age based on cardiovascular features (28), with the GPR model emerging as the most accurate approach in a large cohort of healthy individuals. Here, we assess the potential of this model to indicate cardiovascular risk by measuring deviations from the healthy aging trajectory.

Using deep learning, Attia et al. (54), and Strodtthoff et al. (55) estimated chronological age based on short 12-lead ECG signals both achieving an MAE of 6.9 years. Attia et al. (54) reported that those patients, whose predicted age was >7 yr higher than their chronological age, were more likely to be diagnosed on follow-up with cardiovascular diseases such as hypertension and coronary disease. Similarly, Lima et al. (56) used deep neural networks to estimate age based on raw ECG traces with an MAE of 8–10 yr. In their study, individuals whose estimated age exceeded their chronological age by >8 yr had significantly higher mortality risk. Deep neural networks enable fully automated analysis by using raw ECG signals as input and autonomously learning to extract relevant features, thereby eliminating the need for manual preprocessing or feature engineering. Deep learning approaches can capture complex nonlinear relationships between cardiovascular endpoints and risk. However, their “black-box” nature and high data requirements may limit clinical interpretability and generalizability (57). Ensemble methods such as random forests or *XGBoost* similarly offer strong nonlinear modeling capabilities and robust performance on tabular data but tend to require larger datasets and provide less straightforward physiological interpretability (58, 59). In contrast, GPR provides robust predictions even in relatively

Table 1. Cardiovascular risk factors in the low- and high-risk groups using a deviation of 0.5% from normative risk as threshold

Factors	Low CVR (n = 50)	High CVR (n = 50)	P Value
Age, yr	51.3 ± 13.8	52.6 ± 12.3	0.620
Sex, m/w	34%/66%	52%/48%	0.069
Systolic blood pressure, mmHg	104.6 ± 10.2	132.7 ± 16.9	<0.001
Body mass index, kg/m ²	23.6 ± 2.9	26.8 ± 3.9	<0.001
Smoker, yes/no	0%/100%	26%/74%	<0.001
Framingham risk score, %	5.17 ± 4.73	12.62 ± 8.09	<0.001
Framingham normative risk, %	7.29 ± 5.67	8.01 ± 5.52	0.522
Regular exercise, yes/no	74%/26%	72%/28%	0.822
1–2 h/wk	40%	38%	
3–4 h/wk	28%	24%	
5–6 h/wk	0%	10%	
>6 h/wk	6%	0%	
Depressive symptoms (BDI score)	5.0 ± 5.9	4.3 ± 4.9	0.213

The sample size was fixed at $n = 50$ per group. P values were obtained from t tests for continuous variables or χ^2 tests for dichotomous variables; data are presented as mean ± standard deviation. BDI, Beck Depression Inventory.

Cardiovascular Autonomic Age in testing samples with high and low cardiovascular risk

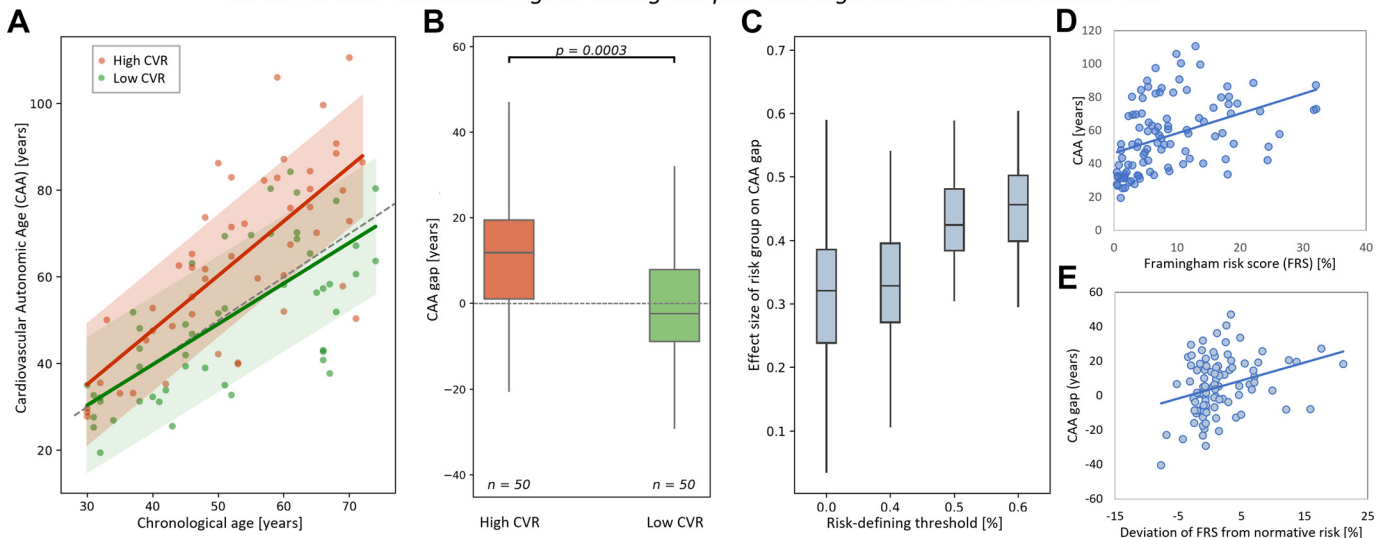


Figure 3. The cardiovascular autonomic age (CAA) gap of participants with high cardiovascular risk (high CVR) and low cardiovascular risk (low CVR) as assessed by a Framingham risk score of $\pm 0.5\%$ above and below normative risk. The sample size was fixed at $n = 50$ per group. P values and effect sizes were obtained from t tests. *A*: CAA in the high-CVR group (red) and low-CVR group (green) as a function of chronological age. Shaded areas represent the standard deviation of data points from the linear fit. *B*: mean CAA gap in high- and low-CVR groups. On average, high-risk participants showed an increased CAA gap of +11.1 years, whereas low-risk participants showed a mean CAA gap of -0.9 yr. *C*: distribution of Cohen's d effect sizes for the CAA gap comparison between risk groups across different thresholds used to define low and high CVR. *D*: scatter plot of the CAA gap vs. Framingham risk score, showing a positive correlation across participants. *E*: scatter plot of the CAA gap vs. deviation from normative risk, also showing a positive correlation.

small cohorts due to its smooth functional form and inherent ability to quantify predictive uncertainty (60, 61).

Although these studies highlight ML's potential for cardiovascular risk assessment through age estimation, our approach extends this concept by enabling the model to learn from a broader physiological basis. Specifically, we incorporate vascular indices and measures of cardiovascular coupling, which are highly sensitive to aging-related changes. With aging, even in the absence of disease, large elastic arteries such as the aorta and carotid arteries become stiffer in both humans and animal models. Stiffening of arterial walls, containing baroreceptors, may compromise their sensory function, hindering the baroreflex mechanism (62).

Notably, the three most influential features in chronological age prediction were 1) the pulse reflection time, 2) pulse transit time, and 3) baroreflex sensitivity. All these parameters are closely linked to arterial stiffness, which progressively accelerates pulsatile blood flow with increasing age (63). Although these indicators were particularly relevant for the age estimation model, diastolic blood pressure and pulse pressure had a comparatively lower impact, even though it is a widely used risk marker and contributed to CVR assessment in our study using the Framingham algorithm.

The average CAA gap indicated that healthy individuals with high CVR appeared from a cardiovascular perspective 11 yr older than expected. In contrast, the low-CVR group had a negative CAA gap of 1 yr, suggesting advanced cardiovascular autonomic aging in those at increased risk for cardiovascular events. In the low-CVR group, the linear fit had a slope of less than one, meaning the estimated age increased by <1 yr for every additional year of chronological age. The decelerated aging might be due to better overall cardiovascular health persisting over

a lifetime. Conversely, the high-CVR group showed a steeper slope (1.3), suggesting accelerated aging processes, with CAA increasing by 1.3 yr for every additional year of chronological age.

Previous research has demonstrated that individuals with elevated Framingham risk scores or obesity-related risk stratifications typically experience cardiovascular disease onset 5–10 yr earlier than those at low risk (18, 22). In this context, the observed CAA gap of approximately 11 yr in the high-risk group may reflect a comparable temporal shift in cardiovascular aging, indicating that autonomic dysregulation captured by the CAA gap could precede clinically manifest disease by several years. The derived CAA might serve as a comprehensive measure of autonomic status and as an independent risk marker that is easy to interpret. This is similar to "vascular age" which has been described as clear and easy to understand by patients rather than an abstract mathematical construct (64). It has been demonstrated that using intelligible risk markers can motivate a population to adopt healthier lifestyles and improve CVR. Lopez-Gonzalez et al. (65) have shown in a randomized clinical trial of 3,000 subjects that expressing cardiovascular risk in terms of years of age ("heart age") leads to decreases in risk scores including BMI reductions, compared with the use of traditional percentage-based markers.

The CAA gap differs fundamentally from established markers like heart age and vascular age, which are typically based on long-term risk factors or imaging of structural changes (e.g., coronary artery calcium and carotid intima-media thickness). Vascular age, for example, can be derived either from population-based imaging norms or from risk models calibrated to structural data (Groenewegen et al. 27). In contrast, the CAA gap relies on short-term cardiovascular

time series data and reflects functional autonomic regulation, rather than structural damage or cumulative risk exposure. This makes it highly sensitive to early, possibly reversible dysregulation that established risk models may miss, especially in younger individuals. Furthermore, CAA can be estimated at rest, noninvasively and without the need for bloodwork or imaging. Since it can be obtained from physiological recordings, the method could, in principle, be implemented using wearable or ambulatory devices for repeated assessments of cardiovascular function over time.

Our study has several limitations that need to be noted. Although we investigated over a thousand subjects, especially at older ages, a rather small amount of data was available. Especially, as the Framingham risk score is validated in an age >30 yr of age, balancing age distribution of the training and the test sets was not possible. However, recruitment of participants of an advanced age without suffering from cardiovascular, neurological, or psychiatric disorder is very complicated. Furthermore, cognitive impairment, sensory loss, and changes in mobility might introduce a selection bias in our study. Although cardiovascular and autonomic aging are known to follow nonlinear trajectories, these inflection points may not be detectable in our results due to the smoothing nature of the GPR model and the limited number of subjects. Longitudinal studies are required in the future to track progression of CAA alongside chronological aging. Finally, the present study is limited by the absence of follow-up data on cardiovascular morbidity and mortality, which would provide the most direct evidence of the prognostic value of the CAA gap.

DATA AVAILABILITY

The data used for training the model is publicly available at physionet.org (<https://physionet.org/content/autonomic-aging-cardiovascular/1.0.0/>).

SUPPLEMENTAL MATERIAL

Supplemental Table S1: <https://doi.org/10.5281/zenodo.17353169>.

GRANTS

This research was funded by the German Research Foundation (DFG, SCHU 3432/2-1, and CR 994/2-1) and the Interdisciplinary Center for Clinical Research, Jena (AMSP17 and MSP17).

DISCLOSURES

No conflicts of interest, financial or otherwise, are declared by the authors.

AUTHOR CONTRIBUTIONS

A.S. and K.-J.B. conceived and designed research; A.S. performed experiments; A.S. and Y.G. analyzed data; A.S., Y.G., M.G., F.d.I.C., D.G., I.D., M.O., C.G., and K.-J.B. interpreted results of experiments; A.S. and Y.G. prepared figures; A.S. and Y.G. drafted manuscript; A.S., D.G., I.D., M.O., C.G., and K.-J.B. edited and revised manuscript; A.S., Y.G., M.G., F.d.I.C., D.G., I.D., M.O., C.G., and K.-J.B. approved final version of manuscript.

REFERENCES

1. **Global Burden of Cardiovascular Diseases and Risks 2023 Collaborators.** Global, regional, and national burden of cardiovascular diseases and risk factors in 204 countries and territories, 1990–2023. *J Am Coll Cardiol* 24: S0735-1097(25)07428-5, 2025. doi:10.1016/j.jacc.2025.08.015.
2. **Dai X, Hummel SL, Salazar JB, Taffet GE, Zieman S, Schwartz JB.** Cardiovascular physiology in the older adults. *J Geriatr Cardiol* 12: 196–201, 2015. doi:10.11909/j.issn.1671-5411.2015.03.015.
3. **Laitinen T, Hartikainen J, Vanninen E, Niskanen L, Geelen G, Länsimies E.** Age and gender dependency of baroreflex sensitivity in healthy subjects. *J Appl Physiol* (1985) 84: 576–583, 1998. doi:10.1152/japplphysiol.1998.84.2.576.
4. **Boettger MK, Schulz S, Berger S, Tancer M, Yeragani VK, Voss A, Bär KJ.** Influence of age on linear and nonlinear measures of autonomic cardiovascular modulation. *Ann Noninvasive Electrocardiol* 15: 165–174, 2010. doi:10.1111/j.1542-474X.2010.00358.x.
5. **Voss A, Heitmann A, Schroeder R, Peters A, Perz S.** Short-term heart rate variability–age dependence in healthy subjects. *Physiol Meas* 33: 1289–1311, 2012. doi:10.1088/0967-3334/33/8/1289.
6. **Laitinen T, Niskanen L, Geelen G, Länsimies E, Hartikainen J.** Age dependency of cardiovascular autonomic responses to head-up tilt in healthy subjects. *J Appl Physiol* (1985) 96: 2333–2340, 2004. doi:10.1152/japplphysiol.00444.2003.
7. **Schumann A, Gupta Y, Gerstorf D, Demuth I, Bär KJ.** Sex differences in the age-related decrease of spontaneous baroreflex function in healthy individuals. *Am J Physiol Hear Circ Physiol* 326: H158–H165, 2024. doi:10.1152/ajpheart.00648.2023.
8. **Monahan KD.** Effect of aging on baroreflex function in humans. *Am J Physiol Regul Integr Comp Physiol* 293: R3–R12, 2007. doi:10.1152/ajpregu.00031.2007.
9. **Steinsaltz D, Patten H, Bester D, Rehkopf D.** Short-term and mid-term blood pressure variability and long-term mortality. *Am J Cardiol* 234: 71–78, 2025. doi:10.1016/j.amjcard.2024.10.005.
10. **Rothwell PM, Howard SC, Dolan E, O'Brien E, Dobson JE, Dahlöf B, Sever PS, Poulter NR.** Prognostic significance of visit-to-visit variability, maximum systolic blood pressure, and episodic hypertension. *Lancet* 375: 895–905, 2010. doi:10.1016/S0140-6736(10)60308-X.
11. **Herrera P, Soljoo S, Stefanovski D, Goldberger JJ, Haigney MC, Punjabi NM.** Habitual sleep duration and QT variability index: correlates of ventricular repolarization lability and all-cause mortality. *Heart Rhythm* 25: S1547-5271(25)02783-3, 2025. doi:10.1016/j.hrthm.2025.08.029.
12. **Thayer JF, Yamamoto SS, Brosschot JF.** The relationship of autonomic imbalance, heart rate variability and cardiovascular disease risk factors. *Int J Cardiol* 141: 122–131, 2010. doi:10.1016/j.ijcard.2009.09.543.
13. **Dekker JM, Crow RS, Folsom AR, Hannan PJ, Liao D, Swenne CA, Schouten EG.** Low heart rate variability in a 2-minute rhythm strip predicts risk of coronary heart disease and mortality from several causes: the ARIC study. *Circulation* 102: 1239–1244, 2000. doi:10.1161/01.CIR.102.11.1239.
14. **Tsuji H, Larson MG, Venditti FJ, Manders ES, Evans JC, Feldman CL, Levy D.** Impact of reduced heart rate variability on risk for cardiac events. *Circulation* 94: 2850–2855, 1996. doi:10.1161/01.CIR.94.11.2850.
15. **Sessa F, Anna V, Messina G, Cibelli G, Monda V, Marsala G, Roberto M, Biondi A, Cascio O, Bertozi G, Pisanelli D, Maglietta F, Messina A, Mollica MP, Salerno M.** Heart rate variability as predictive factor for sudden cardiac death. *Aging (Albany NY)* 10: 166–177, 2018. doi:10.18632/aging.101386.
16. **Hillebrand S, Gast KB, de Mutsert R, Swenne CA, Jukema JW, Middeldorp S, Rosendaal FR, Dekkers OM.** Heart rate variability and first cardiovascular event in populations without known cardiovascular disease: Meta-analysis and dose-response meta-regression. *Europace* 15: 742–749, 2013. doi:10.1093/europace/eus341.
17. **Grassi G, Drager LF.** Sympathetic overactivity, hypertension and cardiovascular disease: state of the art. *Curr Med Res Opin* 40: 5–13, 2024. doi:10.1080/03007995.2024.2305248.
18. **D'Agostino RB Sr., Vasan RS, Pencina MJ, Wolf PA, Cobain M, Massaro JM, Kannel WB.** General cardiovascular risk profile for use

in primary care: the Framingham Heart Study. *Circulation* 117: 743–753, 2008. doi:10.1161/CIRCULATIONAHA.107.699579.

19. Green BB, Anderson ML, Cook AJ, Catz S, Fishman PA, McClure JB, Reid R. Using body mass index data in the electronic health record to calculate cardiovascular risk. *Am J Prev Med* 42: 342–347, 2012. doi:10.1016/j.amepre.2011.12.009.
20. Gaziano TA, Young CR, Fitzmaurice G, Atwood S, Gaziano JM. Laboratory-based versus non-laboratory-based method for assessment of cardiovascular disease risk: the NHANES I Follow-up Study cohort. *Lancet* 371: 923–931, 2008. doi:10.1016/S0140-6736(08)60418-3.
21. Wilson PW, D'Agostino RB, Levy D, Belanger AM, Silbershatz H, Kannel WB. Prediction of coronary heart disease using risk factor categories. *Circulation* 97: 1837–1847, 1998. doi:10.1161/01.cir.97.18.1837.
22. Hubert HB, Feinleib M, McNamara PM, Castelli WP. Obesity as an independent risk factor for cardiovascular disease: a 26-year follow-up of participants in the Framingham Heart Study. *Circulation* 67: 968–977, 1983. doi:10.1161/01.CIR.67.5.968.
23. Cooney MT, Vartiainen E, Laatikainen T, De Bacquer D, McGorrian C, Dudina A, Graham I; SCORE and FINRISK investigators. Cardiovascular risk age: concepts and practicalities. *Heart* 98: 941–946, 2012. doi:10.1136/heartjnl-2011-301478.
24. McClelland RL, Nasir K, Budoff M, Blumenthal RS, Kronmal RA. Arterial Age as a function of coronary artery calcium (from the Multi-Ethnic Study of Atherosclerosis [MESA]). *Am J Cardiol* 103: 59–63, 2009. doi:10.1016/j.amjcard.2008.08.031.
25. Blaha MJ, Naazie IN, Cainzos-Achirica M, Dardari ZA, DeFilippis AP, McClelland RL, Mirbolouk M, Orimoloye OA, Dzaye O, Nasir K, Page JH. Derivation of a coronary age calculator using traditional risk factors and coronary artery calcium: the multi-ethnic study of atherosclerosis. *J Am Heart Assoc* 10: e019351, 2021.
26. Cuende JI, Cuende N, Calaveras-Lagartos J. How to calculate vascular age with the SCORE project scales: A new method of cardiovascular risk evaluation. *Eur Heart J* 31: 2351–2358, 2010. doi:10.1093/euroheartj/ehq205.
27. Groenewegen KA, Den Ruijter HM, Pasterkamp G, Polak JF, Bots ML, Peters SAE. Vascular age to determine cardiovascular disease risk: a systematic review of its concepts, definitions, and clinical applications. *Eur J Prev Cardiol* 23: 264–274, 2016. doi:10.1177/2047487314566999.
28. Schumann A, Gaser C, Sabeghi R, Schulze PC, Festag S, Spreckelsen C, Bär KJ. Using machine learning to estimate the calendar age based on autonomic cardiovascular function. *Front Aging Neurosci* 14: 1–10, 2023. doi:10.3389/fnagi.2022.899249.
29. Schumann A, Bär KJ. Autonomic aging—a dataset to quantify changes of cardiovascular autonomic function during healthy aging. *Sci Data* 9: 95–95, 2022. doi:10.1038/s41597-022-01202-y.
30. Malik M, Bigger J, Camm A, Kleiger R. Heart rate variability: standards of measurement, physiological interpretation and clinical use. Task Force of the European Society of Cardiology and the North American Society of Pacing and Electrophysiology. *Eur Heart J* 17: 354–381, 1996.
31. Bauer A, Kantelhardt JW, Barthel P, Schneider R, Mäkkilä T, Ulm K, Hnatkova K, Schömg A, Huikuri H, Bunde A, Malik M, Schmidt G. Deceleration capacity of heart rate as a predictor of mortality after myocardial infarction: cohort study. *Lancet* 367: 1674–1681, 2006. doi:10.1016/S0140-6736(06)68735-7.
32. Rényi A. On measures of entropy and information. *4th Berkeley Symposium on Mathematical Statistics and Probability*. Berkeley, CA, 1961, vol. 4, p. 547–561.
33. Richman JS, Moorman JR. Physiological time-series analysis using approximate entropy and sample entropy maturity in premature infants. Physiological time-series analysis using approximate entropy and sample entropy. *Am J Physiol Hear Circ Physiol* 278: H2039–H2049, 2000. doi:10.1152/ajpheart.2000.278.6.H2039.
34. Baumert M, Baier V, Haueisen J, Wessel N, Meyerfeldt U, Schirdewan A, Voss A. Forecasting of life-threatening arrhythmias using the compression entropy of heart rate. *Methods Inf Med* 43: 202–206, 2004.
35. Hodes M, Salerno D, Erlien D. Bazett's QT correction reviewed: evidence that a linear QT correction for heart rate is better. *J Am Coll Cardiol* 1: 694, 1983.
36. Berger RD. QT Variability. *J Electrocardiol* 36, Suppl: 83–87, 2003. doi:10.1016/j.jelectrocard.2003.09.019.
37. Floras JS. Blood pressure variability: a novel and important risk factor. *Can J Cardiol* 29: 557–563, 2013. doi:10.1016/j.cjca.2013.02.012.
38. Malberg H, Wessel N, Schirdewan A, Osterziel KJ, Voss A. Dual sequence method for analysis of spontaneous baroreceptor reflex sensitivity in patients with dilated cardiomyopathy. *Z Kardiol* 88: 331–337, 1999. doi:10.1007/s003920050294.
39. Robbe HWJ, Mulder LJM, Rüddel H, Langewitz WA, Veldman JBP, Mulder G. Assessment of baroreceptor reflex sensitivity by means of spectral analysis. *Hypertension* 10: 538–543, 1987. doi:10.1161/01.hyp.10.5.538.
40. Baumert M, Walther T, Hopfe J, Stepan H, Faber R, Voss A. Joint symbolic dynamic analysis of beat-to-beat interactions of heart rate and systolic blood pressure in normal pregnancy. *Med Biol Eng Comput* 40: 241–245, 2002. doi:10.1007/BF02348131.
41. Fischer C, Glos M, Penzel T, Fietze I. Extended algorithm for real-time pulse waveform segmentation and artifact detection in photoplethysmograms. *Somnologie* 21: 110–120, 2017. doi:10.1007/s11818-017-0115-7.
42. Lange A, Marie G, De Cole JH. Commentary: Correction procedures in brain-age prediction. *Neuroimage Clin* 26: 24–26, 2020. doi:10.1016/j.nicl.2020.102229.
43. Cole JH, Ritchie SJ, Bastin ME, Valdés Hernández MC, Muñoz Maniega S, Royle N, Corley J, Pattie A, Harris SE, Zhang Q, Wray NR, Redmond P, Marioni RE, Starr JM, Cox SR, Wardlaw JM, Sharp DJ, Deary IJ. Brain age predicts mortality. *Mol Psychiatry* 23: 1385–1392, 2018. doi:10.1038/mp.2017.62.
44. Lundberg SM, Erion G, Chen H, DeGrave A, Prutkin JM, Nair B, Katz R, Himmelfarb J, Bansal N, Lee SI. From local explanations to global understanding with explainable AI for trees. *Nat Mach Intell* 2: 56–67, 2020. doi:10.1038/s42256-019-0138-9.
45. Cohen J. A power primer. *Psychol Bull* 112: 155–159, 1992. doi:10.1037/0033-2950.112.1.155.
46. Koch M. Artificial intelligence is becoming natural. *Cell* 173: 531–533, 2018. doi:10.1016/j.cell.2018.04.007.
47. Chen M, Hao Y, Hwang K, Wang L, Wang L. Disease prediction by machine learning from healthcare communities. *IEEE Access* 5: 8869–8879, 2017. doi:10.1109/ACCESS.2017.2694446.
48. Sevakula RK, Au-Yeung WTM, Singh JP, Heist EK, Isselbacher EM, Armondas AA. State-of-the-art machine learning techniques aiming to improve patient outcomes pertaining to the cardiovascular system. *J Am Heart Assoc* 9: e013924, 2020. doi:10.1161/JAHA.119.013924.
49. Min M, Egli C, Dulai AS, Sivamani RK. Critical review of aging clocks and factors that may influence the pace of aging. *Front Aging* 5: 1487260–1487210, 2020. doi:10.3389/fragi.2024.1487260.
50. López-Otín C, Blasco MA, Partridge L, Serrano M, Kroemer G. Hallmarks of aging: an expanding universe. *Cell* 186: 243–278, 2023. doi:10.1016/j.cell.2022.11.001.
51. Teschendorff AE, Horvath S. Epigenetic ageing clocks: statistical methods and emerging computational challenges. *Nat Rev Genet* 26: 350–368, 2025. doi:10.1038/s41576-024-00807-w.
52. Xia X, Wang Y, Yu Z, Chen J, Han JDJ. Assessing the rate of aging to monitor aging itself. *Ageing Res Rev* 69: 101350, 2021. doi:10.1016/j.arr.2021.101350.
53. Huang H, Chen Y, Xu W, Cao L, Qian K, Bischof E, Kennedy BK, Pu J. Decoding aging clocks: new insights from metabolomics. *Cell Metab* 37: 34–58, 2025. doi:10.1016/j.cmet.2024.11.007.
54. Atta ZI, Friedman PA, Noseworthy PA, Lopez-Jimenez F, Ladewig DJ, Satam G, Pellikka PA, Munger TM, Asirvatham SJ, Scott CG, Carter RE, Kapa S. Age and sex estimation using artificial intelligence from standard 12-lead ECGs. *Circ Arrhythm Electrophysiol* 12: e007284, 2019. doi:10.1161/CIRCEP.119.007284.
55. Strodthoff N, Wagner P, Schaeffter T, Samek W. Deep learning for ECG analysis: benchmarks and insights from PTB-XL. *IEEE J Biomed Health Inform* 25: 1519–1528, 2021. doi:10.1109/JBHI.2020.3022989.
56. Lima EM, Ribeiro AH, Paixão GMM, Ribeiro MH, Pinto-Filho MM, Gomes PR, Oliveira DM, Sabino EC, Duncan BB, Giatti L, Barreto SM, Meira W, Schön TB, Ribeiro ALP. Deep neural network-estimated electrocardiographic age as a mortality predictor. *Nat Commun* 12: 5117, 2021. doi:10.1038/s41467-021-25351-7.
57. Karatzas P, Dalakleidi K, Athanasiou M, Nikita KS. Interpretability methods of machine learning algorithms with applications in breast

cancer diagnosis. *Annu Int Conf IEEE Eng Med Biol Soc* 2021: 2310–2313, 2021. doi:[10.1109/EMBC46164.2021.9630556](https://doi.org/10.1109/EMBC46164.2021.9630556).

58. **Marchese Robinson RL, Palczewska A, Palczewski J, Kidley N.** Comparison of the predictive performance and interpretability of random forest and linear models on benchmark data sets. *J Chem Inf Model* 57: 1773–1792, 2017. doi:[10.1021/acs.jcim.6b00753](https://doi.org/10.1021/acs.jcim.6b00753).

59. **Fan Z, Song W, Ke Y, Jia L, Li S, Li JJ, Zhang Y, Lin J, Wang B.** XGBoost-SHAP-based interpretable diagnostic framework for knee osteoarthritis: a population-based retrospective cohort study. *Arthritis Res Ther* 26: 213, 2024. doi:[10.1186/s13075-024-03450-2](https://doi.org/10.1186/s13075-024-03450-2).

60. **Ashrafi P, Sun Y, Davey N, Adams RG, Wilkinson SC, Moss GP.** Model fitting for small skin permeability data sets: hyperparameter optimisation in Gaussian Process Regression. *J Pharm Pharmacol* 70: 361–373, 2018. doi:[10.1111/jphp.12863](https://doi.org/10.1111/jphp.12863).

61. **Caywood MS, Roberts DM, Colombe JB, Greenwald HS, Weiland MZ.** Gaussian process regression for predictive but interpretable machine learning models: an example of predicting mental workload across tasks. *Front Hum Neurosci* 10: 647–619, 2016. doi:[10.3389/fnhum.2016.00647](https://doi.org/10.3389/fnhum.2016.00647).

62. **Monahan KD, Dinenno FA, Seals DR, Clevenger CM, Desouza CA, Tanaka H.** Age-associated changes in cardiovagal baroreflex sensitivity are related to central arterial compliance. *Am J Physiol Hear Circ Physiol* 281: H284–H289, 2001. doi:[10.1152/ajpheart.2001.281.1.H284](https://doi.org/10.1152/ajpheart.2001.281.1.H284).

63. **Mitchell GF, Parise H, Benjamin EJ, Larson MG, Keyes MJ, Vita JA, Vasan RS, Levy D.** Changes in arterial stiffness and wave reflection with advancing age in healthy men and women: the Framingham Heart Study. *Hypertension* 43: 1239–1245, 2004. doi:[10.1161/01.HYP.0000128420.01881.aa](https://doi.org/10.1161/01.HYP.0000128420.01881.aa).

64. **Cuende JI.** Vascular age versus cardiovascular risk: clarifying concepts. *Rev Esp Cardiol (Engl Ed)* 69: 243–246, 2016. doi:[10.1016/j.rec.2015.10.019](https://doi.org/10.1016/j.rec.2015.10.019).

65. **Lopez-Gonzalez AA, Aguiló A, Frontera M, Bennasar-Veny M, Campos I, Vicente-Herrero T, Tomas-Salva M, De Pedro-Gomez J, Tauler P.** Effectiveness of the Heart Age tool for improving modifiable cardiovascular risk factors in a Southern European population: a randomized trial. *Eur J Prev Cardiol* 22: 389–396, 2015. doi:[10.1177/2047487313518479](https://doi.org/10.1177/2047487313518479).